

RESEARCH

Open Access



Identification and experimental verification of a biomarker by combining the unfolded protein response with the immune cells in colon cancer

Yichao Ma^{1,6†}, Jingqiu Zhang^{1,6†}, Chen Wei^{1,6†}, Fei Wang⁴, Hao Ji^{1,6}, Jiahao Zhao^{1,6}, Daorong Wang^{1,2,4,5,6,7}, Xinyue Zhang³ and Dong Tang^{1,2,4,5,6,7*}

Abstract

Background The unfolded protein response (UPR) is associated with immune cells that regulate the biological behavior of tumors. This article aims to combine UPR-associated genes with immune cells to find a prognostic marker and to verify its connection to the UPR.

Methods Univariate cox analysis was used to screen prognostically relevant UPRs and further screened for key UPRs among them by machine learning. ssGSEA was used to calculate immune cell abundance. Univariate cox analysis was used to screen for prognostically relevant immune cells. Multivariate cox analysis was used to calculate UPR_score and Tumor Immune Microenvironment score (TIME_score). WGCNA was used to screen UPR-Immune-related (UI-related) genes. Consensus clustering analysis was used to classify patients into molecular subtype. Based on the UI-related genes, we classified colon adenocarcinoma (COAD) samples by cluster analysis. Single-cell analysis was used to analyze the role of UI-related genes. We detected the function of TIMP1 by cell counting and transwell. Immunoblotting was used to detect whether TIMP1 was regulated by key UPR genes.

Results Combined UPR-related genes and immune cells can determine the prognosis of COAD patients. Cluster analysis showed that UI-related genes were associated with clinical features of COAD. Single-cell analysis revealed that UI-related genes may act through stromal cells. We defined three key UI-related genes by machine learning algorithms. Finally, we found that TIMP1, regulated by key genes of UPR, promoted colon cancer proliferation and metastasis.

Conclusions We found that TIMP1 was a prognostic marker and experimentally confirmed that TIMP1 was regulated by key genes of UPR.

Keywords Unfolded protein response, Immune cells, Colon cancer, Prognostic marker

[†]Yichao Ma, Jingqiu Zhang and Chen Wei contributed equally to this work and share the first authorship.

*Correspondence:
Dong Tang
18952783556@yzu.edu.cn

Full list of author information is available at the end of the article



© The Author(s) 2024. **Open Access** This article is licensed under a Creative Commons Attribution-NonCommercial-NoDerivatives 4.0 International License, which permits any non-commercial use, sharing, distribution and reproduction in any medium or format, as long as you give appropriate credit to the original author(s) and the source, provide a link to the Creative Commons licence, and indicate if you modified the licensed material. You do not have permission under this licence to share adapted material derived from this article or parts of it. The images or other third party material in this article are included in the article's Creative Commons licence, unless indicated otherwise in a credit line to the material. If material is not included in the article's Creative Commons licence and your intended use is not permitted by statutory regulation or exceeds the permitted use, you will need to obtain permission directly from the copyright holder. To view a copy of this licence, visit <http://creativecommons.org/licenses/by-nc-nd/4.0/>.

Introduction

Colon adenocarcinoma (COAD) is currently the second leading cause of cancer-related deaths, and its prevalence and deaths are rapidly increasing [1, 2]. However, the atypical early symptoms of colon cancer patients often lead to delays in diagnosis and treatment and even missed opportunities for surgical intervention [3]. Therefore, it is important to find reliable diagnostic and therapeutic targets. In recent years, although immune checkpoint blockade (ICB) has shown beneficial effects in COAD patients, only a small proportion of patients with high microsatellite instability or mismatch repair defects have responded to ICB [4]. Multi-omics are being used to discover new options and directions for the diagnosis and treatment of colon cancer due to the heterogeneity of the tumor immune microenvironment (TIME) [5].

The unfolded protein response (UPR) primarily involves three transmembrane proteins: ATF6, IRE1 α , and PERK [6]. Several studies have shown that the unfolded protein response influences the malignant progression of tumors by altering their immune microenvironment [7]. The researchers found that ATF6 mediates the macrophage-induced resistance to 5-fluorouracil due to membrane translocation of MRP1 [8]. IRE1 α overexpression can induce apoptosis and enhances adaptive anti-cancer immune surveillance to suppress tumors [9]. Genetic or pharmacological targeting of PERK damages NRF2 signaling in myeloid-derived suppressor cells to induce an antitumor immune response, thereby enhancing the efficacy of immune checkpoint blockade and T-cell immunotherapy [10]. These studies suggest that the UPR may influence tumor progression by altering TIME.

Although UPR affecting the TIME has been extensively studied, however, there are few studies combining them to screen tumor prognosis related markers in COAD. In this study, we screened UPR-related genes and immune cells associated with the prognosis of COAD patients in the TCGA database and then obtained UPR-immune-related genes by Weighted correlation network analysis (WGCNA). We found that UPR-immune-related genes play a role in the tumor microenvironment using single-cell analysis. We further obtained the key genes in UPR-immune-related genes by machine learning algorithm. Finally, we experimentally verified the connection between the core gene and UPR (Fig. 1).

Materials and methods

Data gathering and collation

We downloaded the mRNA data and clinical data of the TCGA COAD cohort through R package “TCGABioLinks” (Version 2.29.6) from the TCGA database (<https://portal.gdc.cancer.gov/>) [11]. The data of GSE39582 [12] were obtained from the GEO database ([\[ncbi.nlm.nih.gov/geo/query/acc.cgi?acc=GSE39582\]\(https://www.ncbi.nlm.nih.gov/geo/query/acc.cgi?acc=GSE39582\)\).](https://www.</p></div><div data-bbox=)

In the TCGA dataset, there were 478 tumor specimens and 41 normal specimens, while the GSE39582 dataset included 419 tumor specimens. The gene set of unfolded protein response was downloaded from the human gene database (www.genecards.org) [13].

Differentially expressed genes (DEGs) analysis

R package “limma” (Version 3.50.3) was used to select DEGs [14]. $|\logFC| > 1$ and an adjusted p -value < 0.05 was used to identify DEGs for WGCNA, while $|\logFC| > 1.5$ and an adjusted p -value < 0.05 to select DEGs for UPRs. A larger sample size is required for WGCNA analysis. At the same time, we would like to screen for genes related to UPR as well as immune cells in a wide range. And when screening for UPRs, we need differential genes with bigger differences in expression to narrow down the range of UPRs for prognostic scoring.

Construction of the prognostic UPR_score

We initially screened the UPRs associated with patient prognosis by the univariate cox analysis (R package “survival”, Version 3.2.13), and further screened them by the lasso cox analysis (R package “glmnet”, Version 4.1.6) and the stepwise cox analysis (R package “My.stepwise”, Version 0.1.0). We calculated the coef values for each gene using the multivariate cox analysis (R package “survival”, Version 3.2.13). The UPR_score was calculated as follows: $UPR_score = \sum (Exp_i * coef_i)$.

Exp $_i$ indicated the expression of the gene in the samples. We finally categorized COAD patients into a high UPR_score group (UPR_score $>$ median value) and a low UPR_score group (UPR_score $<$ median value) based on the median UPR_score.

Construction of the prognostic TIME_score

The gene sets of 28 tumor-infiltrating lymphocytes were acquired from the TISIDB website (<http://cis.hku.hk/TISIDB/download.php>), and the scores of different immune cells were obtained using the ssGSEA algorithm (R package “GSVA”, Version 1.42.0). Subsequently, we calculated the immune cells associated with the patient’s prognosis by univariate cox analysis and the coef values of the immune cells using multivariate cox analysis (R package “survival”, Version 3.2.13). The TIME_score was calculated as follows: $TIME_score = \sum (Scoi * coef_i)$.

Scoi represented the score of immune cells calculated by the ssGSEA algorithm. We finally categorized COAD patients into a high TIME_score group (TIME_score $<$ median value) and a low TIME_score group (TIME_score $>$ median value) based on the median TIME_score.

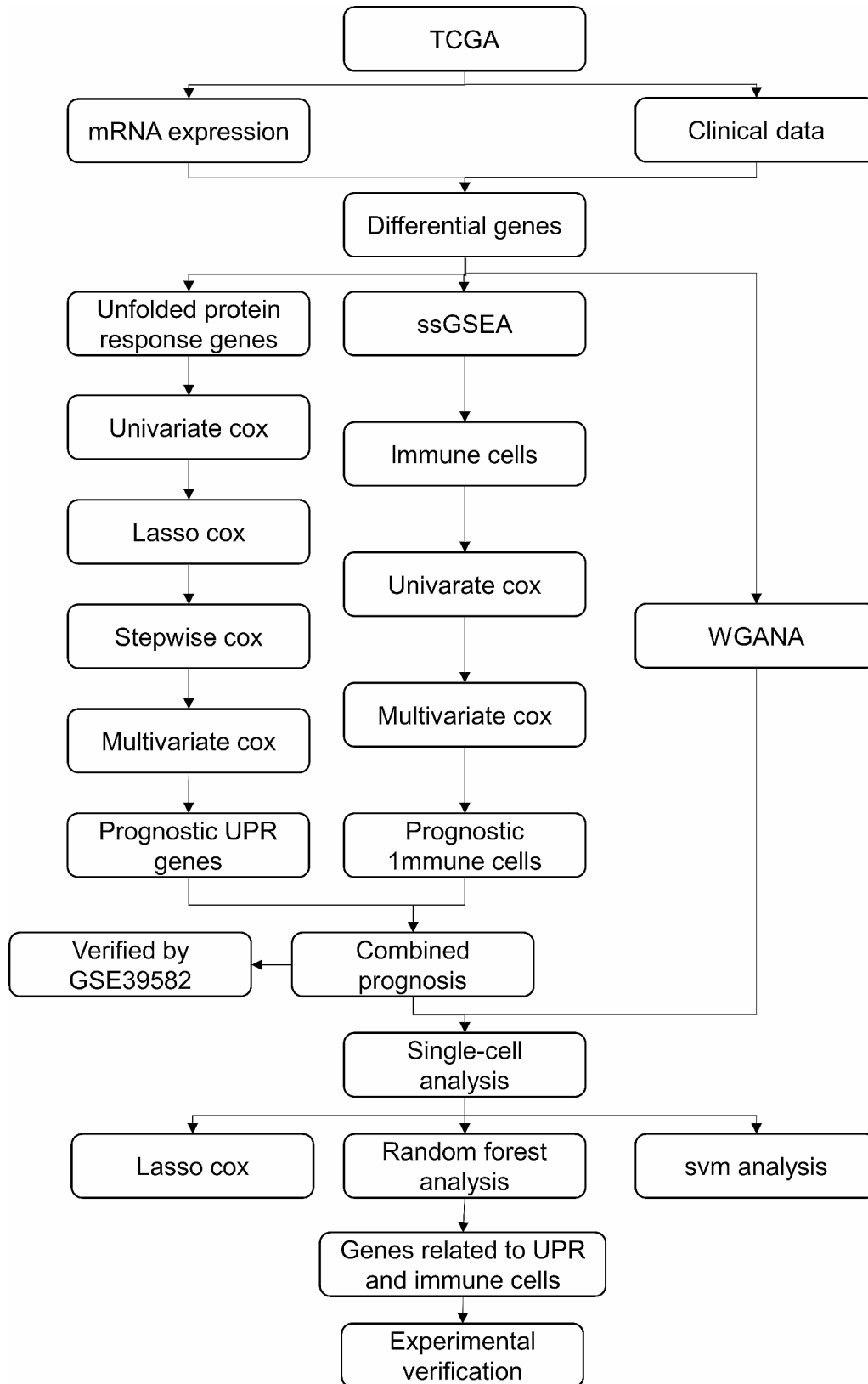


Fig. 1 Workflow of the study design

Kaplan–meier analysis

R package “survminer” (Version 0.4.9) and R package “survival” (Version 3.2.13) was used for Kaplan–Meier analysis based on gene expression. The cutoff value of gene expression was calculated by the `surv_cutpoint` function.

Weighted gene co-expression network analysis (WGCNA)

Analyses of WGCNA were conducted on 5708 DEGs [15] (R package “WGCNA”, Version 1.72.1). The optimal soft threshold power cutoff was set to $R2=0.88$. Weighted gene co-expression networks were constructed based on the optimal values. The degree of correlation between genes was calculated by topological overlap measure (TOM) [16].

We divided the patients into four groups: UPR_high_TIME_high group, UPR_high_TIME_low group, UPR_low_TIME_high group, UPR_low_TIME_low group. We analyzed the correlation between the four groups of patients and the module. We selected the pink modular genes in WGCNA.

Single-cell analysis

We calculate the scores of UPR-immune related genes (UPR-immune-score, UI-score) by the `AddModuleScore` function (R package “Seurat”, Version 4.3.0) in GSE132465 [17]. CellChat was used for evaluating Cellular communication (R package “CellChat”, Version 1.6.1) [18].

Tumor immune dysfunction and exclusion analysis

We employed Tumor Immune Dysfunction and Exclusion (TIDE, <http://tide.dfci.harvard.edu>) to anticipate patient response after immunotherapy.

Screening of hub genes

To further screen the genes in UI-related genes, we used lasso analysis (R package “glmnet”, Version 4.1.6), random forest analysis (R package “randomForest”, Version 4.7.1.1), and support vector machine–recursive feature elimination (SVM-RFE) (R package “e1071”, Version 1.7.13). The grouping settings of the three algorithms are tumor samples and normal samples.

Cell culture

HCT116 and HCT8 were purchased from the Cell Bank of the Chinese Academy of Sciences. We purchased Lenti-X™ 293 T cells from Takara Biomedical Technology Co., Ltd. (Beijing, China). HCT116 cell were cultured in McCoy's 5 A medium, while the Lenti-X™ 293 T and HCT8 cells were cultured in DMEM. The cells were cultured at 37 °C in a humidified incubator with 5% CO₂ and 10% fetal bovine serum, 2 mM L-glutamine, 100 U/mL penicillin, and 100 mg/mL streptomycin.

Lentivirus transduction and plasmid

Lentiviral plasmid (pLKO.1-puro-shATF6, pLKO.1-puro-shPERK, pLKO.1-puro-shIRE1), together with pCMV-dR8.2 and pCMV-VSV-G, were transfected into Lenti-X™ 293 T cells. Cells were selected by 2 µg/mL puromycin for 7 days to establish stable cell strains after transduction. An unrelated shRNA sequence targeting Luciferase was used as a negative control (shLUC). The shRNA sequences are listed as follow:

ATF6 Sense: GCAGCAACCAATTATCAGTTT.

ATF6 Antisense: AAAGTATAATTGGTTGCTGC.

PERK Sense: GTTGTGCTAGCAACCCTAATA.

PERK Antisense: TATTAGGGTTGCTAGCACAAC.

IRE1 Sense: CCCATCAACCTCTCTTCTGTA.

IRE1 Antisense: TACAGAAGAGAGGTTGATGGG.

Luciferase Sense: CGCTGAGTACTTCGAAATGTC.

Luciferase Antisense: GACATTTCTGAAGTACTCAGC G.

Western blot analysis

Using SDS-PAGE, proteins were separated and then electrotransferred to a nitrocellulose membrane. The membranes were blocked with 5% nonfat milk at room temperature and then incubated overnight at 4 °C with primary antibody. Subsequently, the membrane is incubated with the appropriate HRP-labeled secondary antibody. Tanon-5200 chemiluminescence apparatus (Tanon Science & Technology Co. Ltd., Shanghai, China) was used for visualizing bands. The primary antibodies used in this study were ATF6(24169-1-AP, Proteintech, USA), PERK(24390-1-AP, Proteintech, USA), IRE1(27528-1-AP, Proteintech, USA), TIMP1(ab211926, abcam).

Immunohistochemistry (IHC)

In this study, paraffin tissues were obtained from the Northern Jiangsu People's Hospital. The Ethics Committee of the Northern Jiangsu People's Hospital approved the study.

Cell growth curves

Cell growth curves were drawn by counting cells after different culture times.

Statistical analysis

R.4.1.3 and GraphPad Prism 8.0.2 were used to analyze data and visualization. All findings were statistically significant when $P<0.05$.

Results

The combination of UPR and immune cells affected the prognosis of colon cancer patients

2867 differential genes were screened in the TCGA dataset under the condition of $|\log_{2}FC| > 1.5$ and an adjusted p -value < 0.05 (Supplementary File 1). We

obtained 511 UPR-related differential genes after intersecting the differential genes with the UPR-related gene set (Supplementary File 2). Univariate analysis was used to screen for prognostically relevant UPRs. 121 UPR-related genes associated with the prognosis of colon cancer patients were obtained by univariate cox analysis. Lasso cox analysis was used to screen for key prognostically relevant UPRs. After they were used in Lasso cox analysis, we further obtained 30 UPR-associated genes (Fig. 2A-B; Supplementary File 3). Stepwise cox analysis can obtain the final Cox proportional hazards model

for the best candidate. And this model was evaluated by combining several candidate genes with their coefficients as a whole, and we have presented these genes using a bar chart. We performed stepwise cox analysis on the 30 UPR-related genes and obtained the 13 key UPR-related genes (Fig. 2C). We calculated the score for each gene by multivariate cox analysis (Supplementary File 4). We calculated the infiltration abundance of 28 immune cells in the TCGA dataset by ssGSEA and obtained the immune cells associated with the prognosis by univariate cox analysis. The scores of prognostically relevant immune

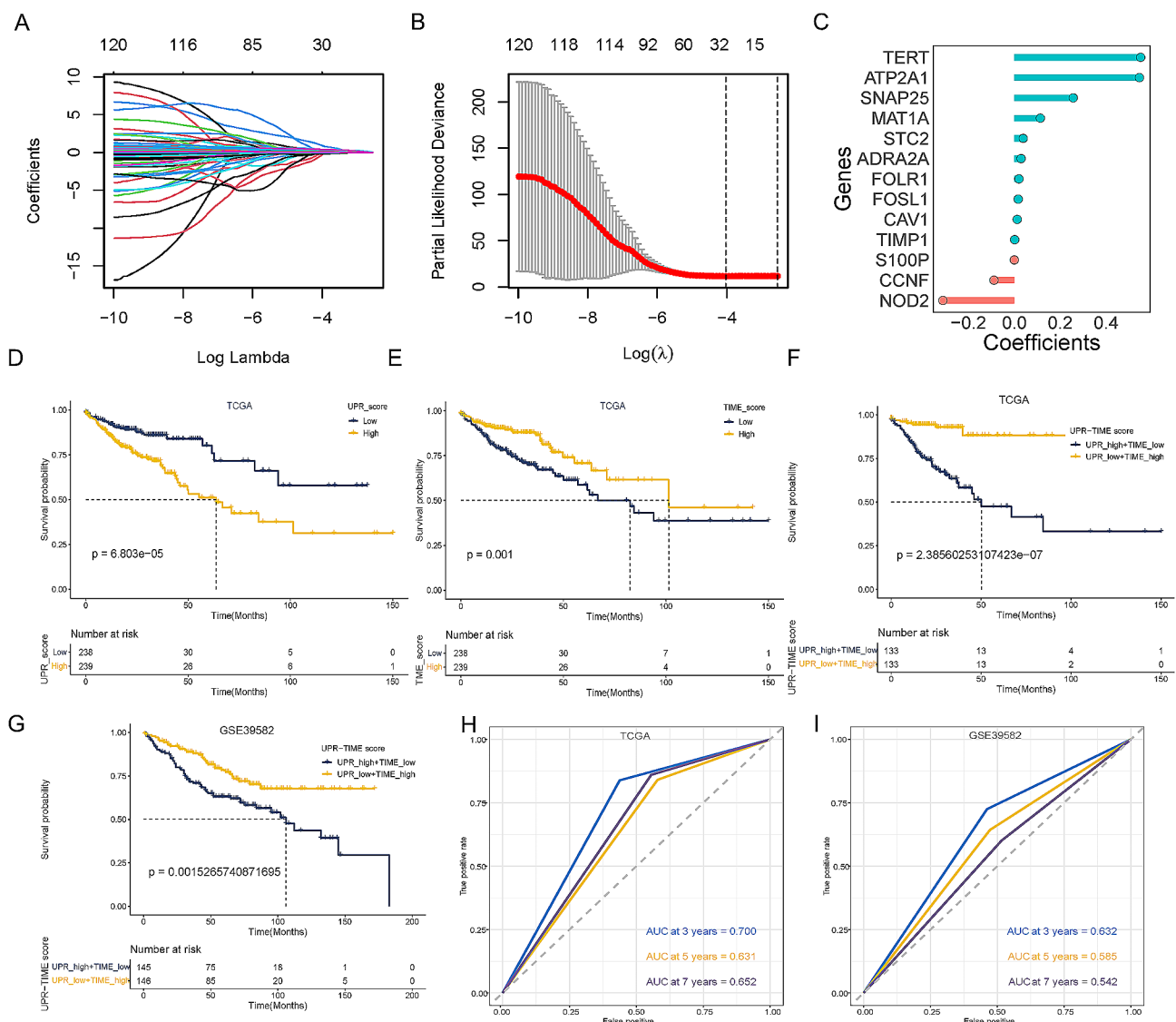


Fig. 2 UPR combined with immune cells to determine the prognosis of colorectal cancer patients. **(A)** Ten-time cross-verification for tuning parameter selection in the LASSO-cox model by R package "glmnet". **(B)** LASSO coefficient profiling by R package "glmnet". **(C)** Genes selected by Stepwise cox analysis (R package "My.stepwise"). **(D)** Survival curve comparing high-risk and low-risk groups based on UPR_score by R package "survival" in TCGA. **(E)** Survival curve comparing high-risk and low-risk groups based on TIME_score by R package "survival" in TCGA. **(F)** Survival curve comparing high-risk and low-risk groups based on TIME_score and UPR_score by R package "survival" in TCGA. **(G)** Survival curve comparing high-risk and low-risk groups based on UPR-TIME score by R package "survival" in GSE39582. **(H)** ROC curve of 1, 3, 5-year survival by R package "timeROC" in TCGA. **(I)** ROC curve of 1, 3, 5-year survival by R package "timeROC" in GSE39582. UPR: unfolded protein response; TCGA: The Cancer Genome Atlas; ROC: Receiver Operating Characteristic; AUC: Area Under the Curve

cells were obtained by multivariate cox (Supplementary File 5). The results of Kaplan-Meier analysis showed that patients in the high UPR_score group had a worse prognosis, which was also observed in the low TIME_score group (Fig. 2D-E). We further categorized patients into four groups by combining UPR_score and TIME_score and found that patients with high UPR_score combined with low TIME_score had a worse prognosis (Fig. 2F). In the GSE39582 dataset, we found the same results (Fig. 2G). The ROC curves showed AUC of 0.7, 0.631, and 0.652 for three, five, and seven years for the TCGA dataset, respectively, whereas they exhibited 0.632, 0.585, and 0.542 in GSE39582 (Fig. 2H-I). These results suggest that UPR may influence the prognosis of colorectal cancer patients in combination with immune cells. However, the AUC of the survival curves was suboptimal and requires further validation.

Screening of prognostically relevant UPR-Immune-related genes by WGCNA and validation of their role in the microenvironment by single-cell data

WGCNA is used to find gene modules composed of highly related genes, summarize these modules using module signature genes or key genes within the module, and correlate the modules with clinical sample traits. We selected the most relevant genes to UPR and TIME through WGCNA, particularly to the UPR_high+TIME_low group and also the UPR_low+TIME_high group. We found that the pink module was most highly correlated with the UPR_high+TIME_low group and least correlated with the UPR_low+TIME_high group. Therefore, we selected 100 genes in the pink module associated with UPR and immune cells based on WGCNA (Fig. 3A, B; Supplementary File 6). We used univariate cox analysis to screen 13 genes associated with the prognosis from the 100 genes (Supplementary File 7). Single-cell data showed significant changes in the proportion of cells in colon cancer compared to normal tissue (Fig. 3C). The UI score was a score calculated using the AddModuleScore function on the screened UPR-immune related genes at the single cell level. We found that the expression of UPR-Immune-related genes was significantly changed in stromal cells and had the largest gap (Fig. 3D). Therefore, we categorized stromal cells into UPR-immune_high (UI_high) stromal cells and UPR-immune_low (UI_low) stromal cells based on UI score. Cell communication analysis was used to observe the communication of the target cell population with other cell populations. By analyzing cell communication, we found that the number of communication between UI_low stromal cells and bone marrow cells was more than that of UI_high stromal cells, whereas the communication strength between UI_high stromal cells and epithelial cells was stronger (Fig. 3E, F). By visualizing the intercellular communication pathways,

we showed that UI_high stromal cells communicated more frequently with other cells in the tumor microenvironment, especially in epithelial cells (Fig. 3G, H).

TIMP1, CAV1, SERPINH1 were further screened from UPR-Immune-related genes by machine learning algorithms

We screened the UPR-immune related genes by WGCNA and screened the key genes related to prognosis by univariate analysis. By single-cell analysis, we verified the role of UPR-immune related genes in the tumor microenvironment. To further search for the key genes, we used machine learning algorithms to screen them. Lasso algorithm, random forest algorithm and SVM algorithm are commonly used for screening genes. We screened eight genes (TIMP1, SERPINH1, NOTCH3, FSTL3, CAV1, SFXN3, SNAI1, S1PR5) by the Lasso algorithm (Fig. 4A-B). We screened six genes (TIMP1, CAV1, SERPINH1, SFXN3, SERPINE1, SNAI1) by random forest algorithm and five genes (TIMP1, SERPINH1, CAV1, NOTCH3, S1PR5) by SVM algorithm (Fig. 4C-E). Through the intersection of the three algorithms, we finally filtered out three core genes (TIMP1, CAV1, SERPINH1) (Fig. 4F). We found that all three genes were associated with the prognosis of colon cancer patients through KM curve analysis (Fig. 4G-L).

Knockdown of TIMP1 inhibited proliferation and migration of colon cancer cell lines

We ultimately screened three core genes (TIMP1, CAV1, SERPINH1) from the UPR-Immune-related genes. We found that TIMP1 appeared during the initial screening process and had the highest importance in the random forest algorithm (Figs. 2C and 5C). Currently, researchers have investigated the link between CAV1, SERPINH1 and the UPR and immune cells. However, although TIMP1 has been studied in relation to immune cells, the relationship between it and the UPR is still unknown. Therefore, in this study, we chose TIMP1 as the study subject. We constructed TIMP1 knockdown colon cancer cell lines (Fig. 5A, B). We found that TIMP1 knockdown decreased the proliferation of HCT116 and HCT8 cell lines (Fig. 5C, D). Meanwhile, we found that TIMP1 knockdown reduced colon cancer cell migration by transwell assay (Fig. 5E). These findings suggested that TIMP1 affected the proliferation and migration of colon cancer cells.

TIMP1 was regulated by key UPR genes

There are three key regulatory genes in the UPR regulatory pathway: ATF6, PERK, and IRE1. To explore the connection between TIMP1 and UPR, we constructed cell lines with knockdown of ATF6, PERK, and IRE1. We found that TIMP1 expression was decreased in HCT116 and HCT8 after knockdown of ATF6, PERK, and IRE1

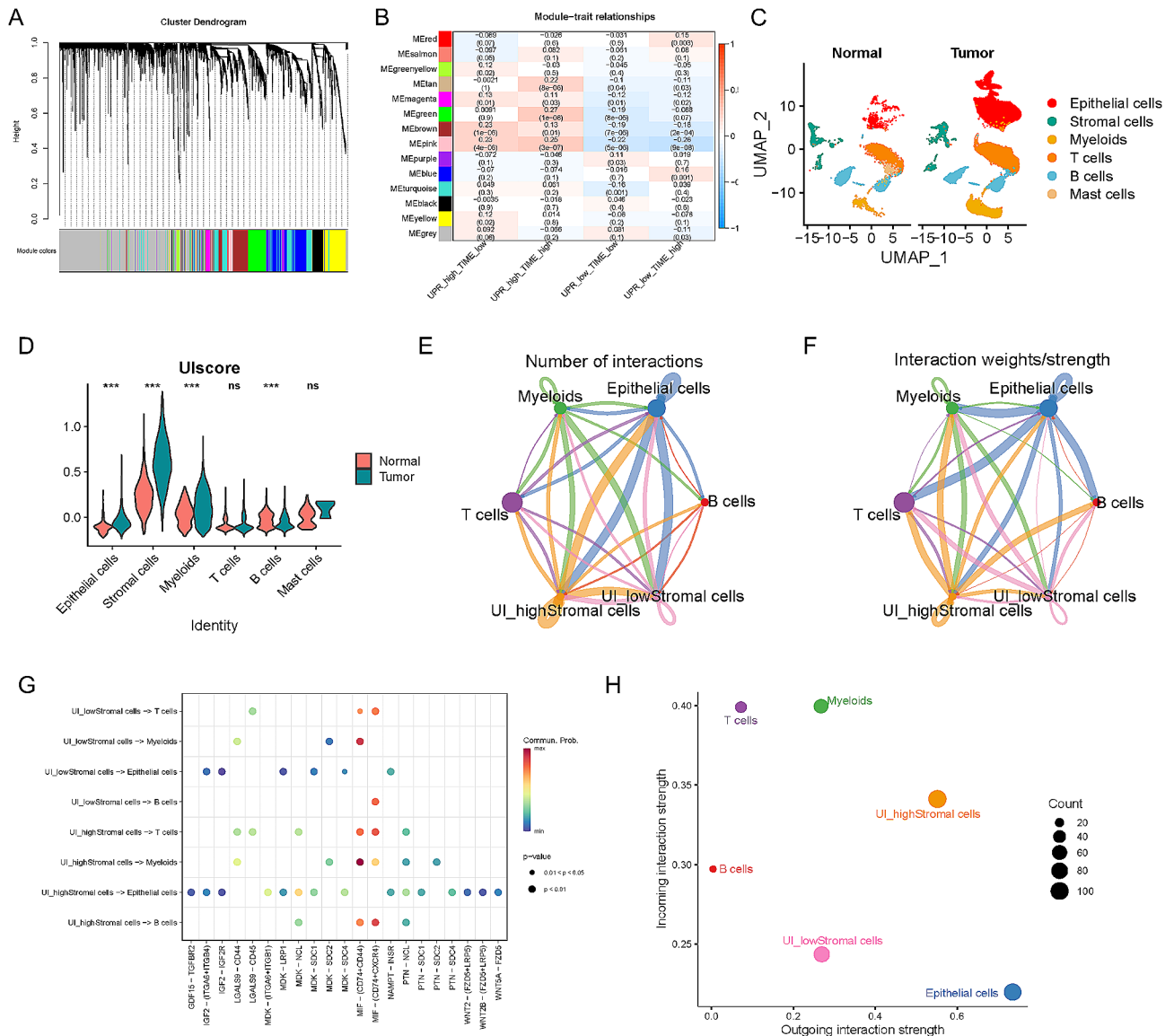


Fig. 3 Screening of prognostically relevant UPR-Immune-related genes by WGCNA and validation of their role in the microenvironment by single-cell data. **(A)** Dynamic Tree and hierarchical clustering modules with different colors by R package “WGCNA”. **(B)** Heatmap of correlation between modules and clinical features by R package “WGCNA”. **(C)** TSNE map of single-cell data by R package “Seurat”. **(D)** Expression of Ulscore in the tumor microenvironment by R package “Seurat”. **(E-F)** The number of cell-to-cell interactions and the total interaction strength by R package “CellChat”. **(G)** Pathway analysis between cells by R package “CellChat”. **(H)** Interaction strength analysis by R package “CellChat”. Ulscore: score of UPR-immune related genes; TSNE: T-distributed Stochastic Neighbor Embedding

(Fig. 6A, B). Immunohistochemistry showed a similarity between TIMP1 and ATF6, PERK, and IRE1 expression in colon cancer tissues (Fig. 6C). These results suggested that TIMP1 was regulated by UPR key genes.

Discussion

In this study, we first found that high UPR_score group and low TIME_score group resulted in poor patient prognosis. Meanwhile, after combining UPR_score and TIME_score, we found that there was a significant difference in the prognosis of patients in the

UPR_high+TIME_low group and the UPR_low+TIME_high group. Therefore, we further screened the genes related to UPR_high+TIME_low group, UPR_low+TIME_high group by WGCNA, and screened the genes among them related to patients’ prognosis by univariate analysis. Next, we verified the relationship between the screened genes and the immune microenvironment using a single-cell dataset. Then, we further narrowed down the screened genes by machine learning algorithm and obtained TIMP1, CAV1, SERPINH1. Currently, researchers have investigated the link between

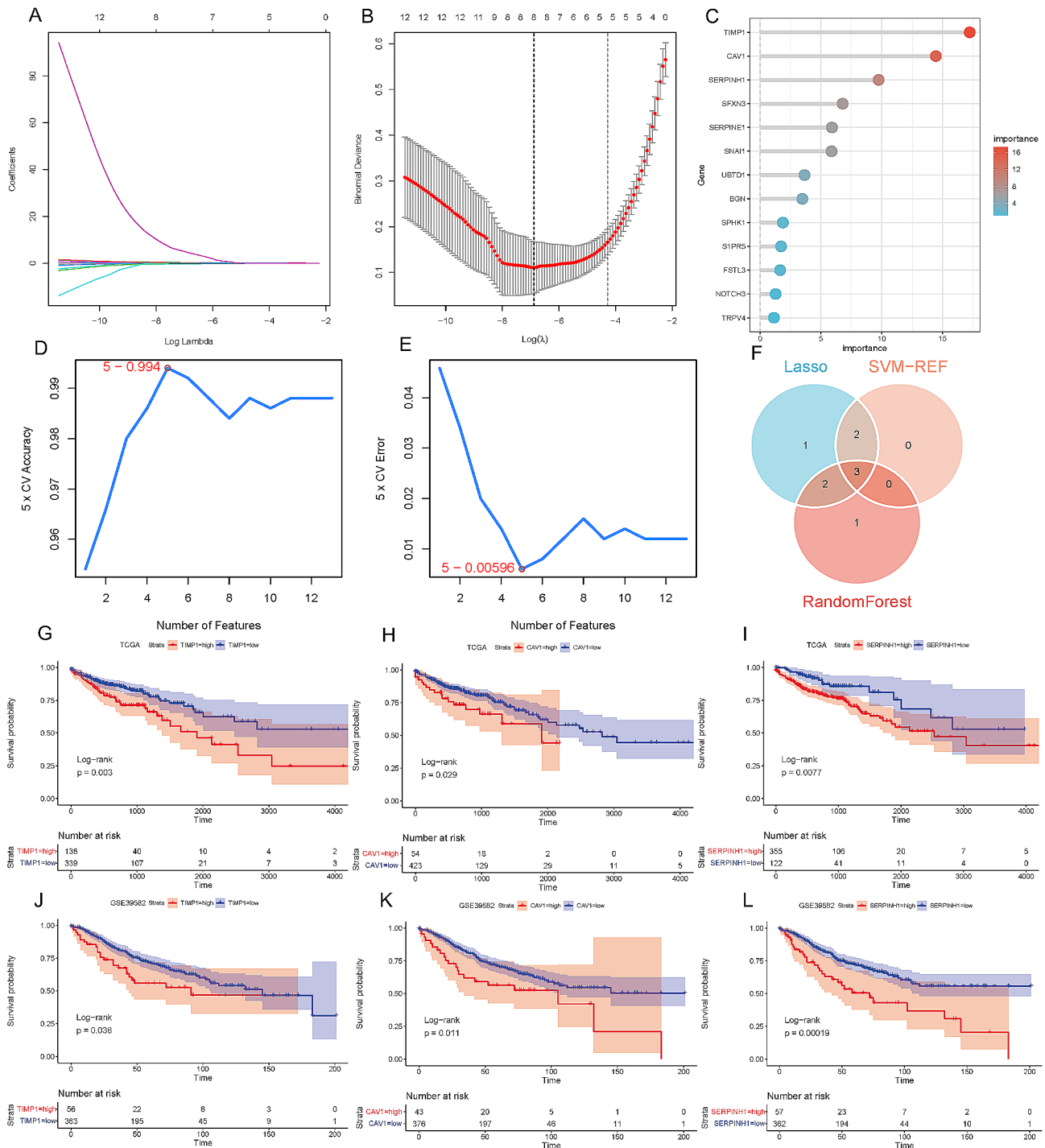


Fig. 4 Hub UPR-immune related genes Screening. **(A)** Ten-time cross-verification for tuning parameter selection in the LASSO-cox model by R package “glmnet”. **(B)** LASSO coefficient profiling by R package “glmnet”. **(C)** Random forest by R package “randomForest”. **(D-E)** SVM-RFE algorithm for feature selection by R package “e1071” and “randomForest”. **(F)** Venn diagram of the LASSO-cox analysis, Random forest analysis, the SVM-RFE algorithm by R package “ggvenn”. **(G-L)** Survival curve at TIMP1, CAV1, SERPINH1 in TCGA and GSE39582 by R package “survival”. LASSO: the Least Absolute Shrinkage and Selection Operator; SVM-RFE: Support Vector Machine–Recursive Feature Elimination

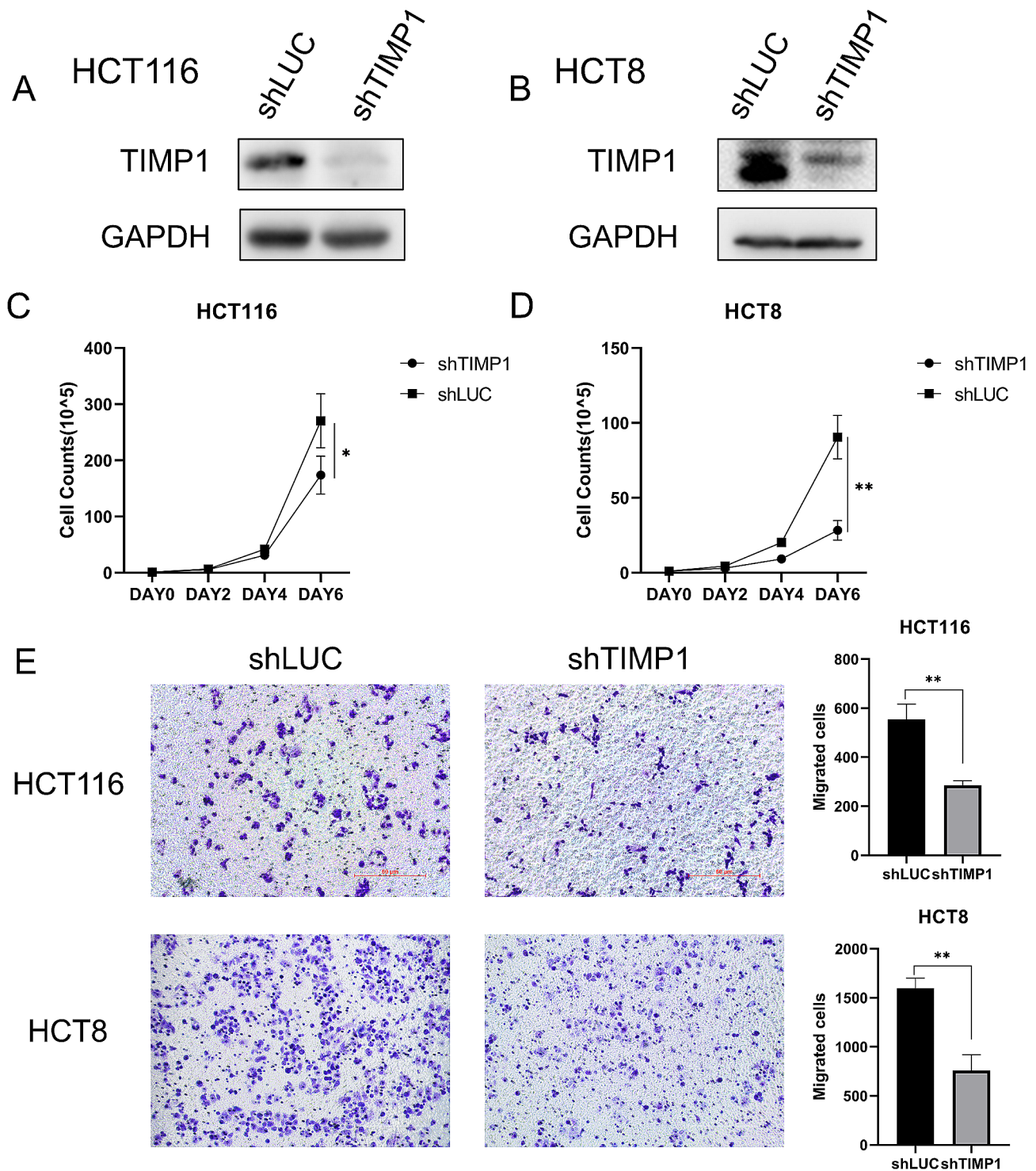


Fig. 5 TIMP1 regulated colorectal cancer growth and migration. (A-B) The levels of TIMP1 protein were determined by western blot analysis in HCT116 and HCT8. (C-D) Cell growth curves. (E) Transwell analysis to examine cell migration

CAV1, SERPINH1 and the UPR and immune cells. However, although TIMP1 has been studied in relation to immune cells, the relationship between it and the UPR is still unknown. Therefore, in this study, we chose TIMP1 as the study subject. We experimentally verified the

function of TIMP1 in colorectal cancer and its relationship with key genes of UPR.

Current studies have shown that cancer cells undergoing UPR can dramatically alter the recruitment and function of immune cells in the tumor microenvironment,

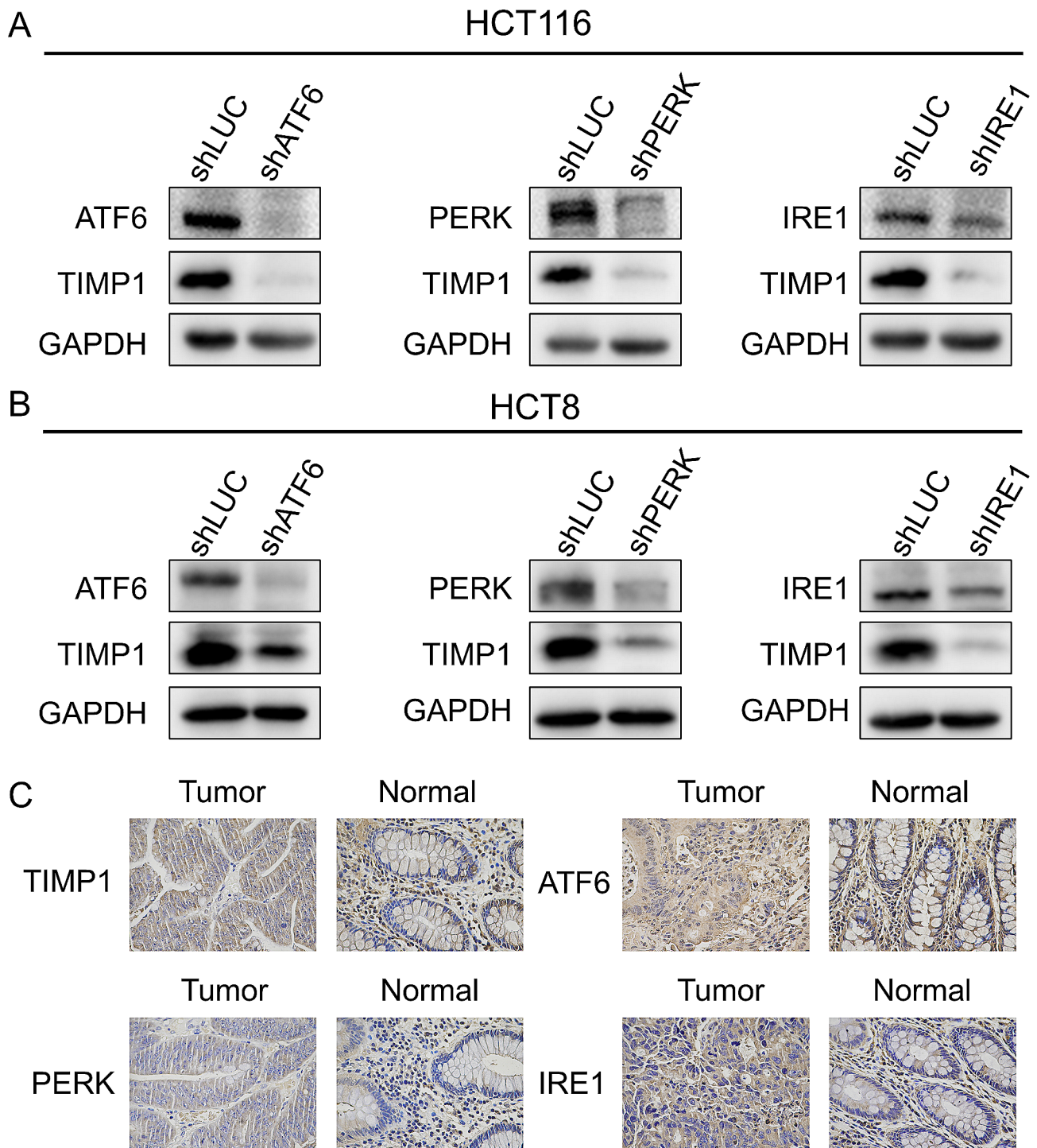


Fig. 6 TIMP1 was regulated by ATF6, PERK, IRE1. **(A-B)** The levels of TIMP1 protein were determined by western blot analysis. **(C)** Immunohistochemistry analysis of TIMP1, ATF6, PERK, and IRE1

coordinating various immune evasion mechanisms to promote malignant progression [19]. The results of this study are consistent with the results of these studies. In the present study, patients with high UPR scores and low TIME scores had a poorer prognosis. After combining the two scores, we found a competitive relationship

between the UPR score and the TIME score, suggesting the promotion of malignant behavior of the tumor by the UPR and the protective effect of immune cells.

We finally screened three key UPR-immune-related genes (TIMP1, CAV1, SERPINH1). CAV1 is localized at the endoplasmic reticulum-mitochondrial interface,

where it impairs the remodeling of endoplasmic reticulum-mitochondrial contacts, reduces protein kinase A signaling, and thereby enhances cell death [20]. Moreover, the researchers found that hypoxia-induced high expression of CAV1 enhanced the metastatic potential of hepatocellular cancer [21]. Anne Schönle et al. found that CAV1 modulates TCR signaling intensity and differentiates regulatory T cells into allogeneic responsive T cells [22]. These studies suggest that CAV1 is associated with the UPR and immune cells, which is consistent with our findings.

SERPINH1 is a molecular companion of collagen that locates in the endoplasmic reticulum and plays a role in the proper folding of collagen [23]. Many studies have shown that HSP47 can promote tumor proliferation and metastasis in cancer cells [24, 25]. Recently, researchers have found that SERPINH1 can interact with IRE1 α to sustain cancer cell growth and enhance their metastatic potential [26, 27]. Interestingly, Takuto Miyamura et al. found that the presence of a large number of SERPINH1-positive fibroblasts in the stroma of lung cancer was a risk factor for postoperative lung cancer recurrence [28]. Similar results were obtained in COAD [29], which provided evidence for the results of the single-cell analysis in this study.

TIMP1 is part of the family of tissue inhibitors of metalloproteinases that inhibit the proteolytic activity of matrix metalloproteinases [30]. Recently, researchers have found that TIMP1 promotes the progression of clear cell renal cell carcinoma by regulating loss-of-nest apoptosis to shape the immunosuppressive microenvironment [31]. TIMP1 overexpression drives lung adenocarcinoma progression through CD63 expression in tumor-associated fibroblasts [32]. Meanwhile, tumor-exposed neutrophils can promote cancer metastasis via a CD90-TIMP1 proximal-paracrine loop [33].

Taken together, we found that CAV1 and SERPINH1 have been studied by researchers in conjunction with the UPR and the immune microenvironment. Meanwhile, TIMP1 has also been shown to be associated with the immune microenvironment. However, the link between TIMP1 and UPR has not yet been studied by researchers. Therefore, we selected TIMP1 as a research object. We verified the function of TIMP1 and found that TIMP1 could promote proliferation and metastasis of colorectal cancer. Then, we knocked down the UPR key gene and found that the expression of TIMP1 decreased after the knockdown of the UPR key gene. This indicated that TIMP1 was regulated by the UPR key gene in colorectal cancer. These results suggested that TIMP1 was a prognostic marker for colorectal cancer regulated by the UPR.

There are many shortcomings in this study. This manuscript attempted to construct a prognostic model, but the prognostic model was not ideal. Also, this manuscript

does not have enough justification for the final selection of genes. Finally, the logic of this manuscript needs to be strengthened.

Conclusion

We found that TIMP1 may be a potential prognostic marker by integrating UPR with immune cells and experimentally confirmed that TIMP1 was regulated by key genes of UPR.

Supplementary Information

The online version contains supplementary material available at <https://doi.org/10.1186/s12885-024-12730-8>.

Supplementary Material 1
Supplementary Material 2
Supplementary Material 3
Supplementary Material 4
Supplementary Material 5
Supplementary Material 6
Supplementary Material 7
Supplementary Material 8

Acknowledgements

The authors thank Zhujiang Dai for his help with data analysis.

Author contributions

YM designed the study. YM, JZ, and CW performed experiments and acquired data. FW, HJ, JZ, and DW contributed to the statistical analysis and interpreted the results. YM and JZ drafted the manuscript and XZ edited it. DT critically revised the article for important intellectual content. All Authors approved the final content for journal submission and publication.

Funding

This work was supported by the Graduate Research- Innovation Project in Jiangsu province [No. SJCX21_1644], the Academic Science and Technology Innovation Fund for College Students [No. 202011117056Y], the Social Development-Health Care Project of Yangzhou, Jiangsu Province [No. YZ2021075], and High-level talent "six one projects" top talent scientific research project of Jiangsu Province [No. LGY2019034], the Graduate Research-Innovation Project in Jiangsu province [No. SJCX22_1816], Social development project of key R ... D plan of Jiangsu Provincial Department of science and technology [No. BE2022773]. The funding bodies had no role in the design of the study; in the collection, analysis, and interpretation of the data; and in the writing the manuscript.

Data availability

The datasets analyzed during the current study are available in the TCGA database (<https://portal.gdc.cancer.gov/>), and the GEO database (<https://www.ncbi.nlm.nih.gov/geo/query/acc.cgi?acc=GSE39582>). The original gel/ blot images are in the supplemental materials.

Declarations

Ethical approval and consent to participate

The patient participating in the study gave informed consent. The Medical Ethics Committee of Northern Jiangsu People's Hospital approved the study on March 17th, 2021. This project was implemented in accordance with the Declaration of Helsinki.

Consent for publication

Not applicable.

Conflict of interest

The authors have no conflicts of interest to declare.

Author details

- ¹Department of General Surgery, Institute of General Surgery, Northern Jiangsu People's Hospital Affiliated to Yangzhou University, Northern Jiangsu People's Hospital, Yangzhou, Jiangsu Province, China
- ²Northern Jiangsu People's Hospital, Clinical Teaching Hospital of Medical School, Nanjing University, Yangzhou 225001, China
- ³College of Bioscience and Biotechnology, Yangzhou University, Yangzhou 225009, Jiangsu, China
- ⁴The Yangzhou School of Clinical Medicine of Dalian Medical University, Northern Jiangsu People's Hospital, Yangzhou 116044, Liaoning, P.R. China
- ⁵The Yangzhou School of Clinical Medicine of Nanjing Medical University, Northern Jiangsu People's Hospital, Yangzhou, China
- ⁶Department of General Surgery, Institute of General Surgery, Northern Jiangsu People's Hospital, Yangzhou, China
- ⁷The Yangzhou Clinical Medical College of Xuzhou Medical University, Northern Jiangsu People's Hospital, Yangzhou, China

Received: 27 March 2024 / Accepted: 30 July 2024

Published online: 08 August 2024

References

1. Dekker E, Tanis PJ, Vleugels JLA, et al. Colorectal cancer. *Lancet*. 2019;394(10207):1467–80. [https://doi.org/10.1016/s0140-6736\(19\)32319-0](https://doi.org/10.1016/s0140-6736(19)32319-0)
2. Siegel RL, Miller KD, Fuchs HE, et al. Cancer statistics, 2022. *CA Cancer J Clin*. 2022;72(1):7–33. <https://doi.org/10.3322/caac.21708>
3. Han L, Chen S, Luan Z, et al. Immune function of colon cancer associated miRNA and target genes. *Front Immunol*. 2023;14:1203070. <https://doi.org/10.3389/fimmu.2023.1203070>
4. Biller LH, Schrag D. Diagnosis and treatment of metastatic colorectal Cancer: a review. *JAMA*. 2021;325(7):669–85. <https://doi.org/10.1001/jama.2021.0106>
5. Bao X, Zhang H, Wu W, et al. Analysis of the molecular nature associated with microsatellite status in colon cancer identifies clinical implications for immunotherapy. *J Immunother Cancer*. 2020;8(2). <https://doi.org/10.1136/jitc-2020-001437>
6. Hetz C, Zhang K, Kaufman RJ. Mechanisms, regulation and functions of the unfolded protein response. *Nat Rev Mol Cell Biol*. 2020;21(8):421–38. <https://doi.org/10.1038/s41580-020-0250-z>
7. Di Conza G, Ho PC, Cubillos-Ruiz JR, et al. Control of immune cell function by the unfolded protein response. *Nat Rev Immunol*. 2023;23(9):546–62. <https://doi.org/10.1038/s41577-023-00838-0>
8. Derycke LD, Bracke ME. N-cadherin in the spotlight of cell-cell adhesion, differentiation, embryogenesis, invasion and signalling. *Int J Dev Biol*. 2004;48(5–6):463–76. <https://doi.org/10.1387/jdb.041793ld>
9. Martinez-Turtos A, Paul R, Grima-Reyes M, et al. IRE1 α overexpression in malignant cells limits tumor progression by inducing an anti-cancer immune response. *Oncoimmunology*. 2022;11(1):2116844. <https://doi.org/10.1080/2162402x.2022.2116844>
10. Mohamed E, Sierra RA, Trillo-Tinoco J, et al. The unfolded protein response Mediator PERK governs myeloid cell-driven immunosuppression in tumors through inhibition of STING Signaling. *Immunity*. 2020;52(4):668–e6827. <https://doi.org/10.1016/j.immuni.2020.03.004>
11. Colaprico A, Silva TC, Olsen C, et al. TCGAAbiolinks: an R/Bioconductor package for integrative analysis of TCGA data. *Nucleic Acids Res*. 2016;44(8):e71. <https://doi.org/10.1093/nar/gkv1507>
12. Marisa L, de Reyniès A, Duval A, et al. Gene expression classification of colon cancer into molecular subtypes: characterization, validation, and prognostic value. *PLoS Med*. 2013;10(5):e1001453. <https://doi.org/10.1371/journal.pmed.1001453>
13. Stelzer G, Rosen N, Plaschkes I, et al. The GeneCards suite: from Gene Data Mining to Disease Genome sequence analyses. *Curr Protoc Bioinf*. 2016;54(1301–). <https://doi.org/10.1002/cpbi.5>
14. Ritchie ME, Phipson B, Wu D, et al. ; limma powers differential expression analyses for RNA-sequencing and microarray studies. *Nucleic Acids Res*. 2015;43(7):e47. <https://doi.org/10.1093/nar/gkv007>
15. Langfelder P, Horvath S. WGCNA: an R package for weighted correlation network analysis. *BMC Bioinformatics*. 2008;9:559. <https://doi.org/10.1186/1471-2105-9-559>
16. Li A, Horvath S. Network neighborhood analysis with the multi-node topological overlap measure. *Bioinformatics*. 2007;23(2):222–31. <https://doi.org/10.1093/bioinformatics/btl581>
17. Lee HO, Hong Y, Etliglu HE, et al. Lineage-dependent gene expression programs influence the immune landscape of colorectal cancer. *Nat Genet*. 2020;52(6):594–603. <https://doi.org/10.1038/s41588-020-0636-z>
18. Jin S, Guerrero-Juarez CF, Zhang L, et al. Inference and analysis of cell-cell communication using CellChat. *Nat Commun*. 2021;12(1):1088. <https://doi.org/10.1038/s41467-021-21246-9>
19. Harnoss JM, Le Thomas A, Reichelt M, et al. IRE1 α disruption in Triple-negative breast Cancer cooperates with antiangiogenic therapy by reversing ER stress adaptation and remodeling the Tumor Microenvironment. *Cancer Res*. 2020;80(11):2368–79. <https://doi.org/10.1158/0008-5472.Can-19-3108>
20. Bravo-Sagua R, Parra V, Ortiz-Sandoval C, et al. Caveolin-1 impairs PKA-DRP1-mediated remodelling of ER-mitochondria communication during the early phase of ER stress. *Cell Death Differ*. 2019;26(7):1195–212. <https://doi.org/10.1038/s41418-018-0197-1>
21. Mao X, Wong SY, Tse EY, et al. Mechanisms through which Hypoxia-Induced Caveolin-1 drives tumorigenesis and metastasis in Hepatocellular Carcinoma. *Cancer Res*. 2016;76(24):7242–53. <https://doi.org/10.1158/0008-5472.Can-16-1031>
22. Schönle A, Hartl FA, Mentzel J, et al. Caveolin-1 regulates TCR signal strength and regulatory T-cell differentiation into alloreactive T cells. *Blood*. 2016;127(15):1930–9. <https://doi.org/10.1182/blood-2015-09-672428>
23. Ito S, Nagata K. Roles of the endoplasmic reticulum-resident, collagen-specific molecular chaperone Hsp47 in vertebrate cells and human disease. *J Biol Chem*. 2019;294(6):2133–41. <https://doi.org/10.1074/jbc.TM118.002812>
24. Zhu J, Xiong G, Fu H, et al. Chaperone Hsp47 drives Malignant Growth and Invasion by modulating an ECM Gene Network. *Cancer Res*. 2015;75(8):1580–91. <https://doi.org/10.1158/0008-5472.Can-14-1027>
25. Xiong G, Chen J, Zhang G, et al. Hsp47 promotes cancer metastasis by enhancing collagen-dependent cancer cell-platelet interaction. *Proc Natl Acad Sci U S A*. 2020;117(7):3748–58. <https://doi.org/10.1073/pnas.1911951117>
26. Yoneda A, Sakai-Sawada K, Minomi K, et al. Heat shock protein 47 maintains Cancer Cell Growth by inhibiting the unfolded protein response transducer IRE1 α . *Mol Cancer Res*. 2020;18(6):847–58. <https://doi.org/10.1158/1541-7786.Mcr-19-0673>
27. Yoneda A, Minomi K, Tamura Y. HSP47 promotes metastasis of breast cancer by interacting with myosin IIA via the unfolded protein response transducer IRE1 α . *Oncogene*. 2020;39(23):4519–37. <https://doi.org/10.1038/s41388-020-1311-7>
28. Miyamura T, Sakamoto N, Ishida K, et al. Presence of heat shock protein 47-positive fibroblasts in cancer stroma is associated with increased risk of postoperative recurrence in patients with lung cancer. *Respir Res*. 2020;21(1):234. <https://doi.org/10.1186/s12931-020-01490-1>
29. Xu CJ, Mikami T, Nakamura T, et al. Tumor budding, myofibroblast proliferation, and fibrosis in obstructing colon carcinoma: the roles of Hsp47 and basic fibroblast growth factor. *Pathol Res Pract*. 2013;209(2):69–74. <https://doi.org/10.1016/j.prp.2012.10.008>
30. Batra J, Robinson J, Soares AS, et al. Matrix metalloproteinase-10 (MMP-10) interaction with tissue inhibitors of metalloproteinases TIMP-1 and TIMP-2: binding studies and crystal structure. *J Biol Chem*. 2012;287(19):15935–46. <https://doi.org/10.1074/jbc.M112.341156>
31. Li Q, Wei K, Zhang X, et al. TIMP1 shapes an immunosuppressive microenvironment by regulating anoikis to promote the progression of clear cell renal cell carcinoma. *Aging*. 2023;15(17):8908–29. <https://doi.org/10.18632/aging.205005>
32. Duch P, Díaz-Valdivia N, Ikemori R, et al. Aberrant TIMP-1 overexpression in tumor-associated fibroblasts drives tumor progression through CD63 in lung adenocarcinoma. *Matrix Biol*. 2022;111:207–25. <https://doi.org/10.1016/j.matbio.2022.06.009>
33. Wang Y, Chen J, Yang L, et al. Tumor-contacted neutrophils promote metastasis by a CD90-TIMP-1 Juxtacrine-Paracrine Loop. *Clin Cancer Res*. 2019;25(6):1957–69. <https://doi.org/10.1158/1078-0432.Ccr-18-2544>

Publisher's Note

Springer Nature remains neutral with regard to jurisdictional claims in published maps and institutional affiliations.